

# Non-ideality of the system $\text{NH}_3\text{-H}_2\text{-N}_2$ . Comparison of equation of state and simulation predictions with experimental data

Luis E. S. de Souza and Ulrich K. Deiters\*

Institut für Physikalische Chemie, Universität zu Köln, Luxemburger Strasse 116, D-50939 Germany

Received 10th June 1999, Accepted 13th July 1999

In this study, experimental  $PVT$  data of pure  $\text{NH}_3$ ,  $\text{H}_2$ ,  $\text{N}_2$  and He are used to extract parameters for a three-parameter semi-empirical equation of state (EOS) for a pure substance and interaction parameters for the exponential-6 (exp-6) potential. For ammonia, the experimental pressure and liquid density at 323 K in the liquid–vapour coexistence region and the experimental density at the same temperature and 9500 bar are taken as inputs in the fitting procedure. For the other species, supercritical data at pressures up to 10 000 bar are selected. It is found that the EOS is not able to simultaneously fit both the liquid–vapour coexistence data and the high pressure region of ammonia. In contrast, the use of Monte Carlo simulations with an optimised set of exp-6 parameters leads to good agreement both at low and high pressure. The quality of the fits to  $\text{H}_2$  and  $\text{N}_2$  data using the EOS is significantly worse than that using the optimised exp-6 potential because the EOS requires physically unreasonable parameters for a good fit. Despite the higher deviations of the EOS results, their corresponding predicted equilibrium constants for the synthesis of ammonia from  $\text{H}_2$  and  $\text{N}_2$  in the industrial range agree just as well with the experimental data. Furthermore, the predicted critical point is slightly closer to the experimental value (a deviation of 10% in the critical temperature). Simulations with the exp-6 potential are performed for the system  $\text{H}_2\text{-He-NH}_3\text{-N}_2$  at pressures and temperatures occurring in the deep atmosphere of Jupiter. Comparison between previous ideal calculations and the simulation predictions indicates that the expected concentration of  $\text{N}_2$  at 2300 K is overestimated by about a factor of three when ideality is assumed.

## 1 Introduction

In this work, the thermodynamical properties of ammonia, hydrogen and nitrogen, as well as those of the mixture containing these species in thermodynamical equilibrium, are modelled in two ways: analytically, using a semi-empirical equation of state (EOS) with three adjustable parameters developed by Deiters,<sup>1–3</sup> and with Monte Carlo simulations, using a model based on isotropic exponential-6 (exp-6) interactions between the species.

Ammonia has been modelled by equations of state as well as interaction potentials of different degrees of complexity. In some cases the models are set to fit well the liquid–vapour behaviour. There is also interest in modelling it at the high pressure for planetary science applications. The literature in the field lacks a more systematic work on the modelling of reacting systems (in the present case, synthesis of ammonia from hydrogen and nitrogen).

This work is a contribution to the evaluation of models as general-purpose approaches, which can treat with reasonable accuracy reacting systems and non-reacting mixtures over a wide range of pressure and temperature, including both the liquid–vapour coexistence region and high pressure (up to  $10^4$  bar) supercritical fluids.

As an application of this work, Monte Carlo (MC) simulations using the exp-6 potential are performed to predict the  $\text{N}_2 : \text{NH}_3$  ratio of a not yet measured system, namely Jupiter's deep atmosphere.

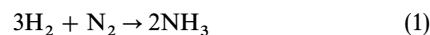
This work is divided into seven parts. After this introduction, the main theoretical aspects of the present work are discussed in Section 2. In Section 3, details about the simula-

tion procedures are given. Section 4 deals with the methods and results of the fits of the two models considered to experimental data. Section 5 shows simulation results in comparison with experimental measurements. In Section 6, MC predictions for the  $\text{N}_2 : \text{NH}_3$  ratio in Jupiter's deep atmosphere are compared with previous ideal gas calculations. Finally, Section 7 contains the discussion and main conclusions of this work.

## 2 Theoretical formulation

### 2.1 Thermodynamical requirements at equilibrium

For the reaction carried out in a one-phase system



at equilibrium the following equation holds:

$$2\mu_3 = 3\mu_1 + \mu_2 \quad (2)$$

where  $\mu_i$  is the chemical potential of the species  $i$  and the subscripts 1, 2 and 3 denote  $\text{H}_2$ ,  $\text{N}_2$  and  $\text{NH}_3$  respectively. The equation above comes from the requirement that at equilibrium the Gibbs free energy change of the system is expressed in terms of the chemical potential and amount of each reacting species as,

$$dG = \mu_1 dn_1 + \mu_2 dn_2 + \mu_3 dn_3 = 0 \quad (3)$$

and the conservation of mass imposes

$$3dn_1 + dn_2 + 2dn_3 = 0 \quad (4)$$

We divide the chemical potential of each species into an ideal part and a residual part in the following way:

$$\mu_i(\mathbf{x}, V_m, T) = \mu_i^{\text{ideal}}(x_i, V_m, T) + \mu_i^{\text{res}}(\mathbf{x}, V_m, T) \quad (5)$$

where  $V_m$ ,  $T$  are the molar volume and temperature of the system and  $\mathbf{x} = \{x_1, x_2, x_3, \dots\}$  is the collection of mole fractions of each species  $j$  in the system, *i.e.*  $x_j = n_j/(n_1 + n_2 + \dots)$ . The ideal part is simply

$$\begin{aligned} \mu_i^{\text{ideal}}(x_i, V_m, T) &= \mu_i^{\text{ideal}}(\rho_i, T) \\ &= \mu_i^{\text{ideal}}(P^\ominus, T) + RT \ln[(\rho_i RT)/P^\ominus] \end{aligned} \quad (6)$$

where  $\rho_i = x_i/V_m = n_i/V$ ,  $R$  = ideal gas constant, and  $P^\ominus$  denotes the reference pressure (often 1 bar). The residual part of the chemical potential is defined by

$$\mu_i^{\text{res}}(\mathbf{x}, V_m, T) = -RT \ln[Z_N/(VZ_{N-1})] \quad (7)$$

where  $Z_N$  is the configuration integral of the  $N$ -molecule system and  $Z_{N-1}$  is the configuration integral of the same system when one  $i$ -molecule is removed.

The expressions above are sufficient to characterize a one-phase mixture in equilibrium. If the system is in liquid–vapour equilibrium, the pressure in the liquid phase equals that in the vapour phase,

$$P_L = P_V \quad (8)$$

and for all species

$$\mu_i^V = \mu_i^L \quad (9)$$

## 2.2 The equation of state

The equation of state used in this work was developed by Deiters<sup>1–3</sup> and has been successfully applied to a variety of systems. It is able to accurately reproduce and predict the phase equilibrium and  $PVT$  behaviour of many fluids. The intent of this work is to check whether it can handle pressures as high as 10000 bar and temperatures far above the critical point and at the same time reproduce the liquid–vapour behaviour.

According to this formulation, the pressure of a pure fluid is given by<sup>1</sup>

$$\begin{aligned} P &= \frac{RT}{V_m} \left[ 1 + c_0 \frac{4\xi - 2\xi^2}{(1 - \xi)^3} \right] - \frac{bRT^*}{V_m^2} \tilde{T}_{\text{eff}} \\ &\times [\exp(1/\tilde{T}_{\text{eff}}) - 1] I_1 \end{aligned} \quad (10)$$

where

$$\tilde{T}_{\text{eff}} = \frac{cT}{T^*} + \frac{\lambda b}{V_m} \quad (11)$$

$$\xi = \frac{\pi\sqrt{2}}{6} \frac{b}{V_m} \quad (12)$$

and  $T^*$ ,  $b$ ,  $c$  are adjustable parameters, with the former two generally expressed in K and  $\text{cm}^3 \text{mol}^{-1}$ , and the latter, related to the anisotropy of the species, is dimensionless.  $I_1$  and  $y$  are functions defined elsewhere,<sup>1–3</sup>  $\lambda/c = -0.06911$  and  $c_0 = 0.6887$ .<sup>1</sup>

In the case of a mixture, mixing rules are of course needed. For the parameter  $c$ ,<sup>3</sup>

$$c = \sum x_i c_i \quad (13)$$

and for  $b$  we adopt the following approximation

$$b = \sum x_i b_i \quad (14)$$

For the parameter  $T^*$ , first we define a dimensionless parameter

$$\gamma = 3(1 - \xi^2) \quad (15)$$

The parameter  $\gamma$  is then used to obtain  $T^*$ :<sup>4</sup>

$$T^* = \left( \sum x_i \sum x_k T_{ik}^* b_{ik}^{2/3} \right) / \left( \sum x_i \sum x_k b_{ik}^{2/3} \right) \quad (16)$$

with  $T_{ik}^* = (T_i^* T_k^*)^{1/2}$  and  $b_{ik} = (b_i + b_k)/2$ .

Another way of generalising eqn. (10) to mixtures is to replace the Carnahan–Starling repulsive term by a hard sphere mixture repulsive term by Mansoori *et al.*<sup>5</sup> As a further refinement, quantum corrections<sup>6</sup> can be added to eqn. (10). Both modifications have been described elsewhere.<sup>6</sup> For the system studied in this work, however, such refinements were found to have only a marginal effect on the results.

## 2.3 The exp-6 potential

The pair potential used in the MC simulations is defined as:

$$\begin{aligned} u(r) &= [\varepsilon/(\alpha - 6)][6 \exp(\alpha(1 - r/r_m)) \\ &\quad - \alpha(r_m/r)^6] \quad \text{for } r > r_c \end{aligned} \quad (17a)$$

$$u(r) = \infty \quad \text{for } r \leq r_c \quad (17b)$$

where  $r$  is the distance between the center of each molecule,  $\varepsilon$  is the depth of the attractive well between them,  $\alpha$  is an adjustable parameter (typically between 10 and 15) and  $r_m$  is the value of  $r$  at the potential minimum. In order to avoid problems in the simulation due to the fact that at very small  $r$  the potential goes to  $-\infty$ , a hard sphere core of diameter  $2r_c$  is introduced in the potential [eqn. (17b)] as common practice.<sup>7</sup>

In dealing with mixtures, the following mixing rules are applied:

$$\varepsilon_{ik} = (\varepsilon_i \varepsilon_k)^{1/2} \quad (18)$$

$$\alpha_{ik} = (\alpha_i + \alpha_k)/2 \quad (19)$$

$$r_m^{ik} = (r_m^i + r_m^k)/2 \quad (20)$$

## 3 Monte Carlo simulations

Three types of MC simulations were performed: (i) one-phase  $NPT$  simulation of a nonreacting substance or mixture; (ii) one-phase  $NPT$  simulation of the reacting  $\text{NH}_3\text{--N}_2\text{--H}_2$  mixture; (iii) two-phase  $NVT$  (Gibbs ensemble) simulation of  $\text{NH}_3$ .

In all cases,  $N = 500$  or 1000 particles were placed in cubic simulation cells with periodic boundary conditions. Long-range corrections for the calculation of the excess internal energy were employed in the usual way,<sup>8</sup> with cutoff at  $L/2$  where  $L$  is the box edge length. For one-phase simulations of nonreacting ammonia during the fitting procedure, we employed  $N = 500$ . In all other cases  $N = 1000$  was used. In case (iii), at the beginning of the simulation 1000 molecules were placed in each box. The sizes of the boxes were chosen so that at the end of the simulation  $N$  was at least about 200 in the vapour phase box. In the particle displacement step, the acceptance of the movement was decided according to the Metropolis criteria.<sup>9</sup> The acceptance ratio was adjusted whenever possible to 0.5.

The Gibbs ensemble simulation was performed following the steps described by Panagiotopoulos *et al.*<sup>10,11</sup> In the particle exchange step, the maximum acceptance ratio was typically 2–3%. Measured vapour and liquid pressures were checked against each other and found to agree.

MC simulations of reacting systems were performed using the so-called reaction ensemble method,<sup>12</sup> which is a generalization of the other types listed above to the case of a reacting system.

Each simulation was divided into blocks, consisting of 25–100 cycles, each one of these containing  $N$  particle dis-

placements, one volume change attempt, as well as particle exchange and reaction attempt steps, whenever applicable. Direct pressure measurements from the virial were made after the particle displacement steps.

A typical simulation required about 3000 cycles after equilibration, except the two-phase simulation, in which about 10000 cycles were employed. Much longer runs were occasionally performed to verify the equilibration of the system.

The reaction attempt step requires ideal free energy data for each species, as defined in eqn. (6). Such data were taken from the TRC Thermodynamic Tables.<sup>13</sup>

## 4 Determination of parameters for the potential and equations of state

### 4.1 Experimental data used in the fits

For ammonia, the following data at 323 K were used: Liquid–vapour region;  $P = 20.33$  bar and liquid density  $0.5629$  g cm<sup>-3</sup>,<sup>14</sup> and  $P = 9500$  bar and density  $0.8117$  g cm<sup>-3</sup>.<sup>15</sup>

Because all models studied have two or three parameters and it is not by any means practical to take too many data points for extracting interaction parameters from MC simulations, only the above data were selected, taking at the same time the liquid–vapour region and an extremely high pressure supercritical point.

For hydrogen, nitrogen and helium, the fits were performed to compressibility factor ( $Z$ ) data, as a function of density and temperature. In the case of hydrogen, 56 data points were generated from a fit to experimental data by Saxena and Fei.<sup>16</sup> In this set  $T$  is between 260 and 800 K and the pressure is up to 10000 bar. For nitrogen, 94 data points by Robertson and Babb<sup>17</sup> were selected, covering the temperature range  $308$  K  $\leq T \leq 673$  K and  $1500$  bar  $\leq P \leq 10000$  bar. For helium, 133 data points for  $98$  K  $\leq T \leq 298$  K and pressure up to 8000 bar were taken from ten Seldam and Biswas.<sup>18</sup>

### 4.2 Parameters for the equation of state

Least-squares fits were performed using eqn. (10), taking  $T^*$  and  $b$  as adjustable parameters. For ammonia, nitrogen and hydrogen, better quality fits are obtained with  $c < 1.0$ , which is not physically acceptable.<sup>1</sup> It is not possible to obtain simultaneous agreement with the two ammonia data points with  $c \geq 1$ . Therefore for the three species  $c$  was set to 1.0 during the fitting procedure. For ammonia, only the liquid–vapour coexistence point was taken to determine the exact values of  $T^*$  and  $b$ . Table 1 lists the selected EOS parameters for the three species, along with the corresponding standard deviations of the compressibility factor residuals,  $\sigma_{\Delta Z}$ .

### 4.3 Parameters for the exp-6 potential

The quality of the exp-6 fit to the experimental data of NH<sub>3</sub>, H<sub>2</sub>, N<sub>2</sub> and He was excellent. The results are listed in Table 2.

For hydrogen, nitrogen and helium, no simulation needed to be performed. Instead, we used the analytical equation of state by Fried and Howard,<sup>7</sup> which is based on Chebyshev polynomials and takes as input both integral equation results (with the hypernetted-mean spherical approximation) and a great number of MC simulation results.

Since the work by Fried and Howard does not address phase equilibrium, it was necessary to perform a series of MC

**Table 2** List of parameters for the exp-6 potential used in this study

Species	$\epsilon/K$	$r_m/\text{\AA}$	$\alpha$	$\sigma_{\Delta Z}$
NH <sub>3</sub>	292.5	3.834	10.7	—
H <sub>2</sub>	24.6	3.371	13.3	0.018
N <sub>2</sub>	101.2	4.062	14.8	0.031
He	11.7	3.193	11.3	0.031

simulations in order to obtain a set of parameters which yield reasonable agreement with the NH<sub>3</sub> experimental data. The algorithm for determining  $\alpha$ ,  $\epsilon$ , and  $r_m$  in this case is:

- (i) Choose an arbitrary  $\alpha$  (between 10 and 15).
- (ii) With the  $\alpha$  chosen in (i), perform a series of  $NPT$  MC simulations at  $T = 323$  K and  $P = 9500$  bar varying  $\epsilon$  and  $r_m$  so that the relation  $r_m = f(\epsilon)$  which yields the correct experimental density under such conditions is determined. Typically,  $r_m$  has a much greater influence on the resulting density than  $\epsilon$ , which reduces considerably the number of simulations needed in this step.
- (iii) Perform a series of Gibbs MC simulations at 323 K in the liquid–vapour region, using  $\alpha$  from step (i) and a set of  $\epsilon$  [with  $r_m$  from step (ii)] in a reasonable region. From the results, estimate which  $(\epsilon, r_m)$  set satisfies the experimental pressure at 323 K in the liquid–vapour coexistence region with  $\alpha$  chosen in (i). Record also the estimated value of the liquid density for the chosen set.
- (iv) Repeat steps (i)–(iii) with other values of  $\alpha$  and, by extrapolation, get the value of  $\alpha$  (and from that the  $\epsilon, r_m$  corresponding set) which yields (besides the correct density and 9500 bar vapour pressure) the correct liquid density at 323 K.

## 5 Comparison of EOS and exp-6 results with experimental data

In this section, the EOS [eqn. (10)] and exp-6 predictions are compared with available experimental data. Figs. 1 and 2 show the liquid–vapour coexistence diagram for non-reacting (pure) ammonia. The experimental critical density, temperature and pressure ( $\rho_c = 0.235$  g cm<sup>-3</sup>,  $T_c = 405.5$  K,  $P_c = 112.8$  bar),<sup>14</sup> is indicated in the figures as a circle. The experimental data point used in the fit is indicated as a star marker. The dotted lines are EOS predictions and the square markers indicate MC exp-6 results. The EOS predicted critical point ( $\rho_c = 0.243$  g cm<sup>-3</sup>,  $T_c = 444.3$  K,  $P_c = 153.6$  bar) is somewhat closer to the experimental value than the MC simulations. In both models, both the critical pressure and the

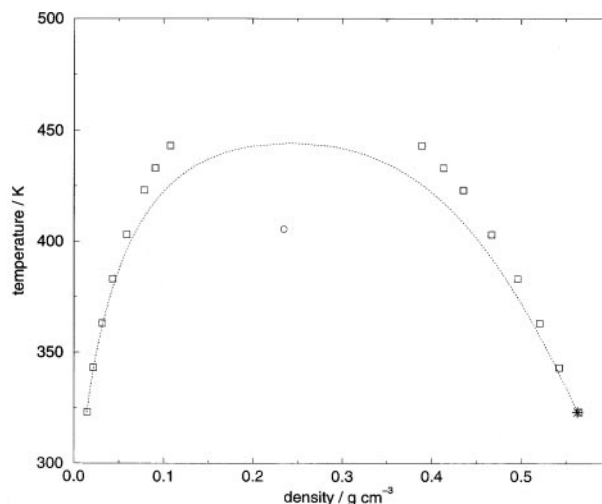


**Fig. 1** Liquid–vapour behaviour of non-reacting ammonia as predicted by using eqn. (10) (dotted line) and by Monte Carlo simulations using an isotropic exp-6 potential (squares). The experimental critical point (circle) and the experimental point in the liquid–vapour region used in the fit (star) are also shown.

**Table 1** List of EOS parameters used in this study [eqn. (10)]

Species	$T^*/K$	$b/\text{cm}^3 \text{ mol}^{-1}$	$c$	$\sigma_{\Delta Z}$
NH <sub>3</sub>	305.2	15.63	1.0	(exact)
H <sub>2</sub>	12.67	8.24	1.0	0.033
N <sub>2</sub>	26.28	17.66	1.0	0.334

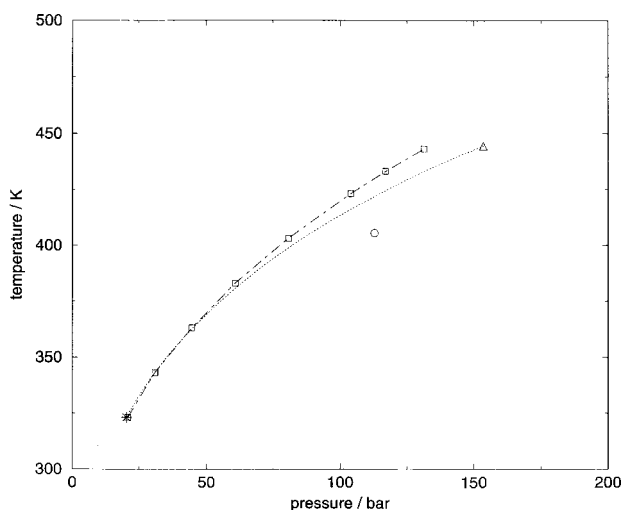
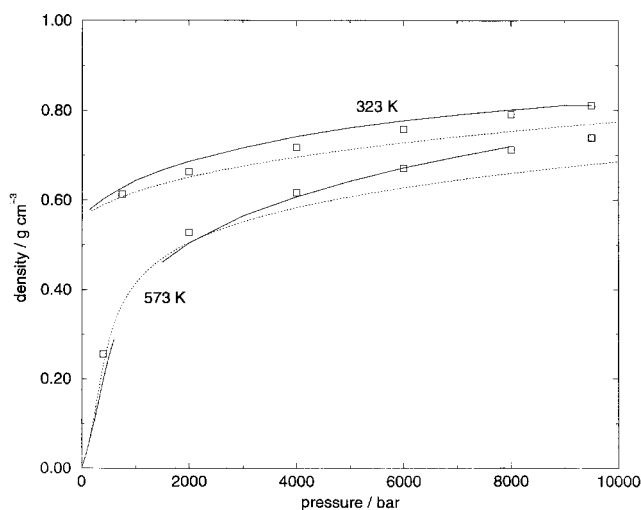


**Fig. 2** Pressure-temperature diagram of non-reacting ammonia in the liquid-vapour coexistence region as predicted by using eqn. (10) (dotted line) and by Monte Carlo simulations using an isotropic exp-6 potential (dot-dashed line with squares). The EOS predicted critical point (triangle), the experimental critical point (circle), the experimental point in the liquid-vapour region used in the fit (star) are also shown.

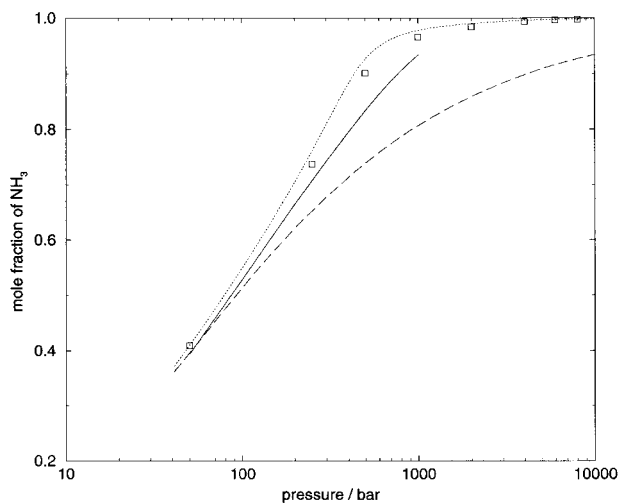
critical temperature are overestimated. Considering that only two data points have been used to adjust the parameters in the exp-6 models and only one for the EOS model, the liquid-vapour ammonia results can be considered fairly good.

Fig. 3 shows the pressure dependence of pure ammonia density at  $T = 323$  and  $573$  K. The experimental data are represented by the solid lines whereas the MC predictions are indicated by square markers and the EOS results are indicated by dotted lines. The agreement between theory and experiment is fairly good, especially for the MC results. It is possible to appreciate the wide pressure range which the simulations are able to reproduce. Not surprisingly, the EOS predictions have a poorer performance at high pressure; the predicted density is underestimated. In setting  $c = 1$ , the best possible agreement at high pressure was aimed at. However, in this region, pressure estimates from density values are still very poor using the EOS model.

EOS and exp-6 parameters for nitrogen and hydrogen have also been determined for making another interesting comparison with experimental data: the pressure and temperature dependence of the ammonia mole fraction in a mixture of



**Fig. 3** Pressure dependence of non-reacting ammonia density at 323 and 573 K. Predicted results using eqn. (10) (dotted lines) and Monte Carlo simulations using an isotropic exp-6 potential (squares) are shown. Experimental measurements are indicated by solid lines for comparison.



**Fig. 4** Pressure dependence of the mole fraction of  $\text{NH}_3$  (in a system at thermodynamical equilibrium with  $\text{H}_2 : \text{N}_2 = 3 : 1$ ) at 573 K. Predicted results using eqn. (10) (dotted line) and Monte Carlo simulations using an isotropic exp-6 potential (squares) are shown. Experimental measurements (solid line) are also shown for comparison. The theoretical results from exclusively ideal gas calculations (dashed line) clearly indicate the significance of the non-ideal part.

$\text{NH}_3$  in thermodynamical equilibrium with 3 : 1  $\text{H}_2/\text{N}_2$ . Figs. 4 and 5 show how well the reaction ensemble MC results (squares) and EOS predictions (dotted lines) agree with the experimental data<sup>14</sup> at 573 and 873 K, which are represented as solid lines. At 573 K (Fig. 4), the MC predictions seem to be slightly more accurate than the EOS predictions. At 873 K (Fig. 5), however, both MC and EOS results are in excellent agreement with each other and with the experimental data. In Figs. 4 and 5 the results obtained for a noninteracting (*i.e.*, ideal) fluid are also shown as long-dashed lines. It is clear that the EOS and exp-6 corrections for non-ideality significantly improve the accuracy of the theoretical predictions as the pressure increases.

## 6 Dissociation of $\text{NH}_3$ in Jupiter's deep atmosphere

Fegley and Lodders have performed extensive calculations of equilibrium constants in Jupiter's deep atmosphere assuming ideality.<sup>19</sup> What is the difference between their results and a

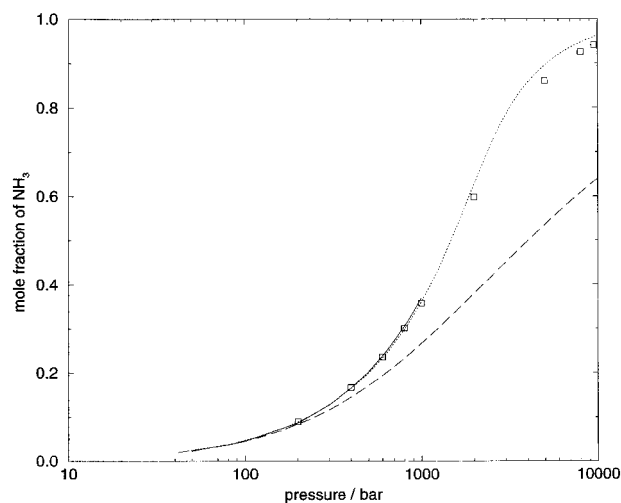


**Fig. 5** Pressure dependence of the mole fraction of  $\text{NH}_3$  (in a system at thermodynamical equilibrium with  $\text{H}_2 : \text{N}_2 = 3 : 1$ ) at 873 K. Predicted results using eqn. (10) (dotted line) and Monte Carlo simulations using an isotropic exp-6 potential (squares) are shown. Experimental measurements (solid line) and ideal gas results (dashed lines) are also shown for comparison.

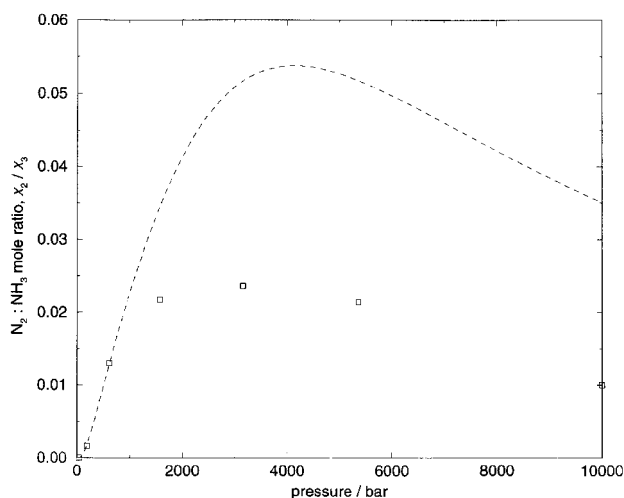


**Fig. 6** Pressure dependence of the  $N_2:NH_3$  mole ratio,  $x_2/x_3$ , in the deep atmosphere of Jupiter. The system is assumed to be in thermodynamical equilibrium with 10% helium and about 90% of hydrogen, with trace amounts of nitrogen. Predicted results assuming ideality (dashed line) and extrapolated results to  $x_2 \rightarrow 0$  from Monte Carlo simulations (squares) are shown along a trajectory toward the center of the planet.

more realistic calculation, which accounts for the non-ideality of the system at high pressures? The answer to this question can be obtained by a reaction ensemble MC simulation. In Jupiter's deep atmosphere, it can be assumed that the mole fraction of  $H_2$  and He are about 0.90 and 0.10 respectively.<sup>19</sup> The relative amount of nitrogen and its compounds is comparatively negligible. In a MC simulation, this would correspond to infinite dilution of  $NH_3$  and  $N_2$  in a mixture of  $H_2$  and He with mole ratio 9 : 1.

Thus, a series of reaction ensemble simulations of the system  $H_2$ -He- $NH_3$ - $N_2$  was performed at selected temperatures between 500 and 2300 K. In the initial conditions,  $N = 1000$ ,  $N_4 = 100$  (the subscript 4 indicates helium) and  $N_3 = 0$ . In each simulation, the effect of the initial ratio of  $N_2:N_1$  and the pressure was verified. Extrapolation of  $x_3^2/(x_1^3x_2)$  to  $N_2:N_1 = 0$  yielded the expected  $x_2:x_3$  ratio at Jupiter's deep atmosphere at a given temperature and pressure, using the values of  $x_{H_2} = x_1$  and  $x_{NH_3} = x_3$  by Fegley and Lodders.<sup>19</sup> Fig. 6 presents the simulation results as a function of pressure, along with the corresponding ideal gas calculations. The same results are plotted in Fig. 7, but as a function of temperature. At 500 K and 38 bar, the system is

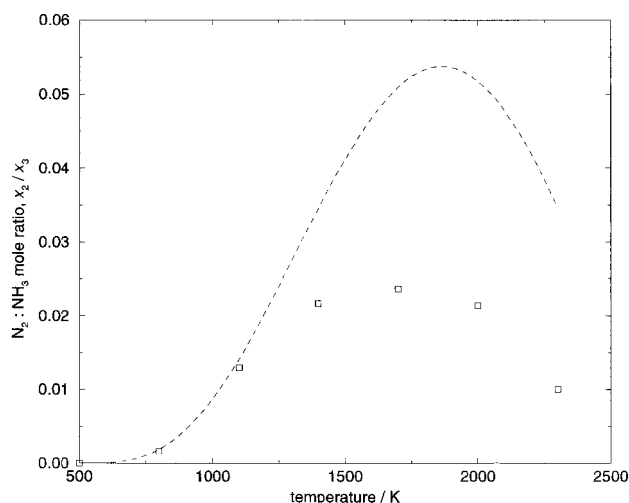


**Fig. 7** The same results shown in Fig. 6 are reproduced here as a function of temperature in Jupiter's deep atmosphere. The pressure-temperature dependence there is taken from the work by Fegley and Lodders.<sup>19</sup>

essentially an ideal gas. On the other hand, the mole fraction of  $N_2$  is about 250% overestimated when ideality is assumed at the highest temperature and pressure point. This makes the detection of the nitrogen species in the deep atmosphere of Jupiter even harder as anticipated by consideration of the ideal gas calculations. An interesting feature shown in Figs. 6 and 7 is that there is a point at which the maximum  $x_2:x_3$  is achieved. This results from the competing effects of temperature and pressure on the chemical equilibrium. High pressure favors the consumption of nitrogen (since there is plenty of hydrogen in Jupiter) whereas high temperature favors the production of nitrogen (and hydrogen) from ammonia. In Jupiter, both pressure and temperature increase along the path to Jupiter's interior.

## 7 Discussion and conclusions

The analytical EOS [eqn. (10)] results indicate that the model is able to semi-quantitatively predict the equation of state of ammonia and the properties of the  $NH_3$ - $N_2$ - $H_2$  mixture over a large temperature and pressure range, including the liquid-vapour coexistence curve. Not surprisingly, the higher the temperature, the better the accuracy of the model because the ideal part contributes relatively more to the thermodynamical properties of the system. Particularly good are the ammonia critical point and mole fraction of ammonia in the industrial range at 873 K. It is necessary to emphasize that only two-parameter equations of state (disregarding  $c$ ) for pure substances have been used. In calculating the properties of the mixture, the parameters were calculated from previously fixed mixing rules and not adjusted in any way to experimental data. The results suggest that the model based on the equation of state [eqn. (10)] is able to give reasonable first estimates of the properties of a high pressure fluid taking only low pressure data in the liquid-vapour coexistence region.

Particular attention needs to be paid to parameter  $c$  though. For ammonia, hydrogen and nitrogen the best choice of  $c$  parameter which is also physically meaningful is 1.0. This value, which is assigned to an isotropic molecule, is required for obtaining an agreement as good as possible with high pressure data. Of course the properties of a fluid at high pressure are more sensitive to the shape of the species which compose the fluid. However, this fact does not imply that high pressure fluids are better modelled as anisotropic. On the contrary, as demonstrated by Belonoshko and Saxena,<sup>20</sup> an isotropic exp-6 potential is able to reproduce the  $PVT$  properties of several fluids at high pressure. Therefore a reasonable interpretation of the apparently higher isotropicity of the species investigated (in particular,  $NH_3$ ) at high pressure is that a good fit using the EOS formulation over a wide range of pressure requires a decrease in  $c$  as the pressure increases, corresponding to a change in "effective" shape of the species in the fluid. Thus, a density dependence of  $c$  could yield a significant improvement of the EOS formulation accuracy for the system studied.

A comparison between the analytical EOS and exp-6 simulation results indicates that the latter is clearly more accurate, despite its weakness in the transition region between low and high pressure. The EOS formulation [eqn. (10)], which is well suited for fitting and predicting fluid properties in the liquid-vapour coexistence curve and its vicinity, is challenged when extreme conditions are studied. Neither the substitution of a hard-sphere mixture repulsion term<sup>5,6</sup> nor the inclusion of quantum corrections<sup>6</sup> changed the EOS results significantly. For pure ammonia,  $H_2$  and  $N_2$ , there is no visible change. For the reacting system, the improved EOS model results are slightly worse at the 573 K. On the other hand, the exp-6 potential has been used to treat high pressure phenomena and is not designed to handle strongly polar or nonspherical molecules. Nor does it account for quantum effects or more

complex interactions. Therefore the clear advantage of the exp-6 modelling compared to the EOS [eqn. (10)] could be attributed to its better self-consistency, along with a very realistic, soft core, potential. However, it is very clear that for more complex systems it is also bound to fail.

It is relevant to point out that the exp-6 potential has been generally applied to supercritical fluids. The results of this work suggest that the application to fluid phase equilibria should be investigated further. Future work in the field involves, for instance, using the isotropic exp-6 potential to investigate systems with strongly polar or chain molecules in the phase equilibrium region. In proposing improvements, it would be desirable to keep its simplicity while obtaining greater flexibility in the treatment of a wider variety of systems.

Finally, equations of state in general are probably the most convenient way to calculate the thermodynamic properties of a system. The fact that the models considered cannot handle one-phase supercritical fluids in a region far above the critical point in pressure and temperature indicates that there is still a lot of work to be done in the field.

### Acknowledgements

L. de S. would like to thank the Alexander von Humboldt Foundation for its support of this work.

### References

- 1 U. Deiters, *Chem. Eng. Sci.*, 1981, **36**, 1139.
- 2 U. Deiters, *Chem. Eng. Sci.*, 1981, **36**, 1147.

- 3 U. Deiters, *Chem. Eng. Sci.*, 1982, **37**, 855.
- 4 U. K. Deiters, *Fluid Phase Equilib.*, 1987, **33**, 267.
- 5 G. A. Mansoori, N. F. Carnahan, K. E. Starling and T. W. Leland, *J. Chem. Phys.*, 1971, **54**, 1523.
- 6 U. K. Deiters, M. Neichel and E. U. Franck, *Ber. Bunsen-Ges. Phys. Chem.*, 1993, **97**, 649.
- 7 L. E. Fried and W. M. Howard, *J. Chem. Phys.*, 1998, **109**, 7338.
- 8 M. P. Allen and D. J. Tildesley, in *Computer Simulation of Liquids*, Oxford University Press, New York, 1991, pp. 64–65.
- 9 M. P. Allen and D. J. Tildesley, in *Computer Simulation of Liquids*, Oxford University Press, New York, 1991, pp. 118–123.
- 10 A. Z. Panagiotopoulos, *Mol. Phys.*, 1987, **61**, 813.
- 11 A. Z. Panagiotopoulos, N. Quirke, M. Stapleton and D. Tildesley, *Mol. Phys.*, 1988, **63**, 527.
- 12 W. R. Smith and B. Triska, *J. Chem. Phys.*, 1994, **100**, 3019.
- 13 In *TRC Thermodynamic Tables—Non-Hydrocarbons*, ed. M. Frenkel, N. M. Gadalla, K. R. Hall, X. Hong, K. N. Marsh and R. C. Wilhoit, Thermodynamics Research Center, The Texas A&M University System, College Station, Texas, 1997, p. x-500.
- 14 H. Bakemeier, T. Huberich, R. Krabetz and W. Liebe, in *Ullmann's Encyclopedia of Industrial Chemistry*, ed. Wolfgang Gerhartz, VCH, Weinheim, 1985, vol. A2, pp. 143–156.
- 15 A. Harlow, G. Wiegand and E. U. Frank, *Ber. Bunsen-Ges. Phys. Chem.*, 1997, **101**, 1461.
- 16 S. K. Saxena and Y. Fei, *Geochim. Cosmochim. Acta*, 1988, **52**, 1195.
- 17 S. L. Robertson and S. E. Babb, Jr., *J. Chem. Phys.*, 1969, **50**, 4560.
- 18 C. A. ten Seldam and S. N. Biswas, *J. Chem. Phys.*, 1992, **96**, 6163.
- 19 B. Fegley, Jr. and K. Lidders, *Icarus*, 1994, **110**, 117.
- 20 A. B. Belonoshko and S. K. Saxena, *Geochim. Cosmochim. Acta*, 1992, **56**, 3611.

Paper 9/04645C